Cement & Concrete Composites 42 (2013) 9–19

Contents lists available at SciVerse ScienceDirect

Cement & Concrete Composites

journal homepage: www.elsevier.com/locate/cemconcomp

Influence of bundle coating on the tensile behavior, bonding, cracking and fluid transport of fabric cement-based composites

D. Dvorkin [a], A. Poursaee [b], A. Peled [c,*], W.J. Weiss [d]

[a] Material Engineering Department, Ben Gurion University of the Negev, Beer Sheva, Israel
[b] Glenn Department of Civil Engineering, Clemson University, Clemson, SC, USA
[c] Structural Engineering Department, Ben Gurion University of the Negev, Beer Sheva, Israel
[d] School of Civil Engineering, Purdue University, West Lafayette, IN, USA

ARTICLE INFO

Article history:
Received 19 July 2012
Received in revised form 13 May 2013
Accepted 16 May 2013
Available online 25 May 2013

Keywords:
Fluid transport
Cement based composite
Carbon fabric
Bonding
Cracking
Tensile properties
Wedge test

ABSTRACT

The goal of this work was to study the mechanical performance and fluid ingress of fabric cement based components made of epoxy coated and non-coated multifilament carbon fabrics. Direct tensile, pullout, and fluid transport tests were performed. Cracking was observed using four test geometries: (i) tensile tests, (ii) pullout tests, (iii) restrained shrinkage tests, and (iv) wedge splitting tests. The results show that coating multifilament carbon yarns improves mechanical behavior and bonding of the composite when compared with non-coated carbon yarn composites. The non-coated carbon systems may be problematic due to poor bonding as well as their potential to permit fluid ingress along the bundle–matrix interface and through the empty spaces between filaments. In addition, it was also found that fabric with coated bundles reduces crack width and develops dense branched network cracks. However, these additional fine cracks were found to increase fluid ingress into the matrix as compared with the plain cement paste.

1. Introduction

Research has shown benefits of using textile fabric reinforcement in cement-based composites (TFRC) in terms of improved tensile strength, toughness, ductility and energy absorption [1–5]. The use of TFRC also allows controlled the crack width, providing a network of fine cracks. The overall mechanical behavior of TFRCs including crack pattern and crack width depends on the fabric geometry, the fabric material, and the nature of yarns made the fabric, either monofilament or multifilament. Further, in the case of multifilament, the behavior may be dependent on whether the bundle is coated or non-coated. Kruger et al. [6] concluded that fabrics with epoxy impregnated bundle of filaments exhibit improved bond resistance in concrete.

Alkali resistant (AR) glass fabrics have been extensively studied for use in TFRC component applications [1]. Carbon textiles have been gaining attention recently as reinforcement for cement-based composites due to their mechanical performance and stability in the aggressive environment in cement paste [7,8]. Zhu et al. [7] reported tensile strength of 5 MPa and toughness of 0.024 MPa for AR glass TFRC element, while the performance of carbon TFRC had strengths of as high as 27 MPa, with 0.35 MPa toughness under the same loading conditions. This point to the benefits in performance of carbon TFRC.

A significant component of the durability of TFRC components is related to their resistance to the transport of fluids into and through the composite. The majority of research on textile fabric reinforced cement-based products has been focused on mechanical properties. It is well known that mechanical behavior and cracking are related. It is typical that composites with better bonding exhibit finer distributed cracks pattern. This is expected to reduce fluid ingress into the composite and improve its durability. Only limited work has been reported on the influence of textile fabric reinforcement on fluid transport into cracked TFRC elements [8,9].

The objective of this work was to study the mechanical performance, crack pattern and fluid ingress of TFRC components reinforced with carbon fabrics. Cracking was measured using several geometries including: (i) direct tensile specimen, (ii) restrained shrinkage specimen, and (iii) wedge splitting specimen. In addition pullout tests were performed to study the bond behavior.

2. Experimental details

2.1. Fabric reinforcement

Commercially available carbon fabrics were used in this study with a mesh form. Multifilament carbon yarns composed from

* Corresponding author. Tel.: +972 8 6479672; fax: +972 8 6479670.
E-mail address: alvpeled@bgu.ac.il (A. Peled).

0958-9465/$ - see front matter © 2013 Elsevier Ltd. All rights reserved.
http://dx.doi.org/10.1016/j.cemconcomp.2013.05.005

12,000 filaments were used to produce the fabrics. Two sets of fabric were prepared and studied:

(i) *Coated carbon fabric* (Fig. 1a): in which the bundle yarns were first coated with epoxy and then used to form the fabric. In this case the bundle is fully coated, i.e., all filaments within the bundle are connected and glued together by epoxy, providing a one unit reinforcing system, when assuming perfect bond between epoxy and filaments.
(ii) *Non-coated carbon fabric* (Fig. 1b): in which no coating was applied to the bundle and the yarns remained free. As a result of the lack of coating there are empty spaces between the filaments (i.e., the filaments are not glued together). Here the reinforcing bundle unit is made of filaments which are separated and slide freely against each other.

Both fabrics had exactly the same structure and were made of the same roving under the same machine and conditions, and the only difference between them was the coating. In both cases the warp bundles (along the length of the fabric) were the reinforcing yarns as presented in Fig. 1.

The carbon fabrics, with and without coating, were tested under direct tensile tests. The average tensile strength of the original non-coated yarn fabric was 1218 MPa with modulus of elasticity of 210 GPa. The coating led to increase of the average tensile strength to 2423 MPa with a slight reduced in the modulus of elasticity to 204 GPa. This improved tensile behavior of the coated fabric was mainly due to bonding of the filaments within the bundle as the polymer connected and glued them together. This connection can provide good stress transfer between filaments during loading, improving the tensile behavior of the coated fabric and its reinforcing ability when part of the cement composite. For the fabric without coating the filaments were separated and therefore transfer stresses by friction only due to sliding against each other, resulting in lower tensile behavior of the fabric.

2.2. Sample preparation and test methods

Several sets of specimen were prepared for the different test methods: (1) direct tensile, (2) pullout, (3) restrained shrinkage, and (4) wedge splitting. For each test a single layer of fabric was placed in between two layers of fresh cement paste. Plain cement paste was used in all cases in order to simplify the system and isolate the influences related to the paste and fabric only on bonding. A type I ordinary portland cement (OPC) was used in all cases. The OPC had a Blaine fineness of 360 m^2/kg and an estimated Bogue phase composition of 60% C_3S, 12% C_2S, 12% C_3A, 7% C_4AF and Na_2O equivalent of 0.72%. The water to cement ratio (w/c) was either 0.40 or 0.42 as noted for the specific experiments.

2.2.1. Direct tension tests

Samples were prepared by one layer of fabric that was placed using hand layup in between two layers of cement paste with a w/c of 0.40. The preparation of the composite was carried out in special mold, resulting in 8 mm thick coupons with a length of 250 mm and a width of 30 mm, respectively. Vibration was applied during the preparation of the specimens to achieve a good penetration of the cement matrix in between the openings of the fabric. The volume fraction of reinforcement was 4% when considering the reinforcing yarns only. The specimens were demolded 1 day after casting and maintained continuously in tap water until testing at age of 21 days. For each fabric type (coated and non-coated) five samples were prepared.

The samples were tested using a closed loop tensile test in an Instron testing machine with constant strain rate of 0.5 mm/min (Fig. 2a). The test was carried out until a 10 mm extension was achieved or until complete failure of the composite occurred. Aluminum plates (with tapered ends) were glued on both specimen faces in the grips region to provide better stress transfer during testing when loaded in the grips. The cracks that developed during the tensile test were recorded by a camera at intervals of 15 s. Average properties were obtained including: the ultimate (maximum) tensile stress (UTS) and energy consumption (calculated as the area under the stress–strain curves). Representative samples were chosen and graphically compared. For each set of specimens an average tensile curve was plotted, the response from the five original tested samples that exhibited the closest behavior to the average was selected. The typical representative curve showed tensile behavior similar to the average one but also included additional details which were impossible to see by the average curve.

2.2.2. Pullout tests

The pullout specimens were prepared using hand lay-up of single fabric layer in the center of cement matrix with a w/c of 0.40. The pulled out yarns within the fabric were the warp yarns. The warp yarns were also the reinforcing yarns in the tension specimens. The width of the fabric in the composite was 10 mm, providing two pulled out yarns during testing. The size of the specimen

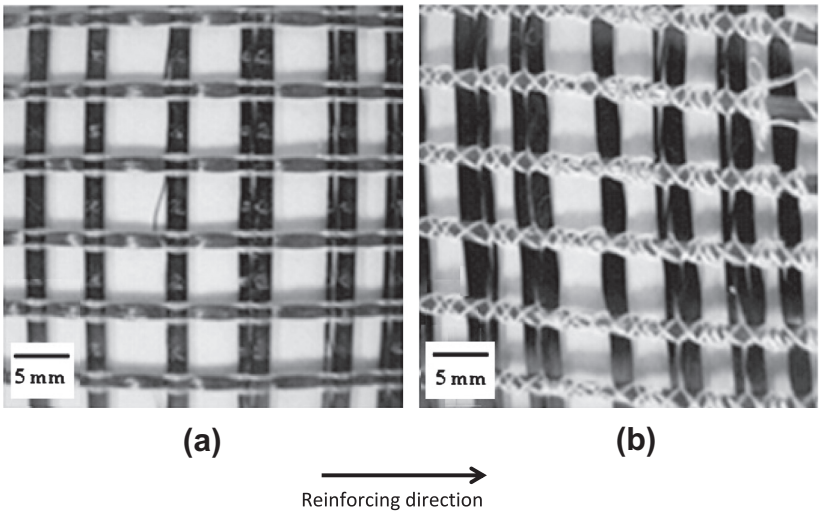

Fig. 1. Carbon fabric systems: (a) coated and (b) non-coated fabrics.

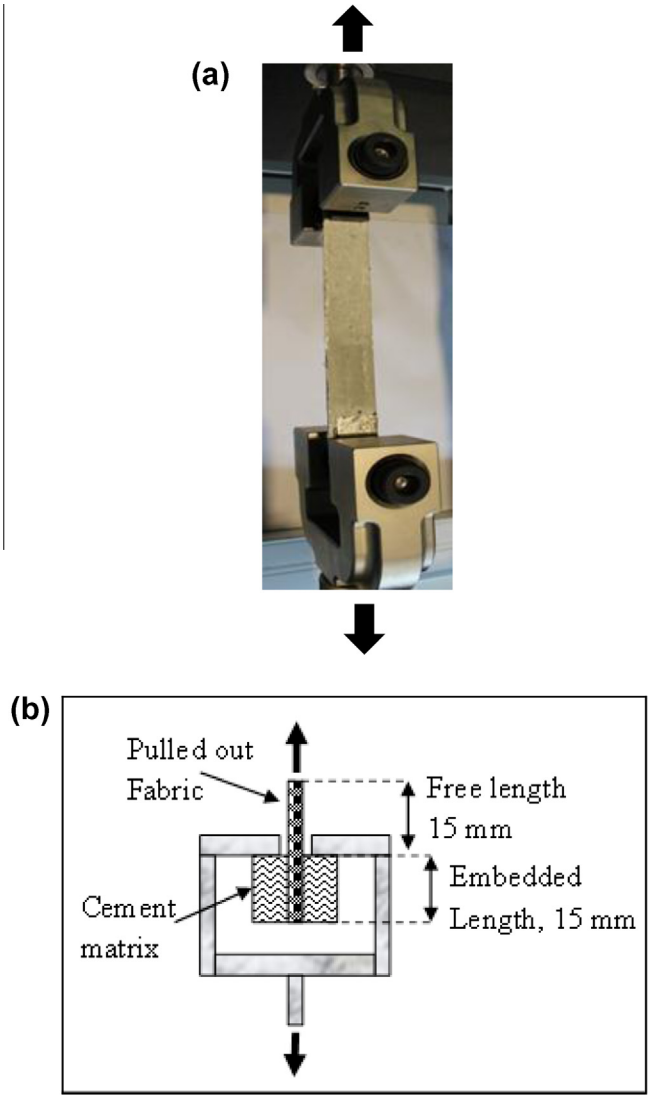

Fig. 2. Tests set up for (a) tensile loading and (b) pullout loading.

was 8 mm thick, 30 mm wide and 15 mm long. The length of the specimen was equal to the embedded length of the individual fabric in the cement matrix. The specimens were demolded 1 day after casting and maintained continuously in tap water until testing at age of 21 days as the tensile specimens. For each fabric type (coated and non-coated) ten samples were prepared.

The evaluation of the bond characteristics of the coated and non-coated reinforcing system was based on pullout tests. The pullout samples were tested with the same strain rate as the tensile test. The pullout test was conducted until 10 mm of slip was attained. The pullout testing set up is presented in Fig. 2b. Two warp yarns were pullout in both cases coated and non-coated. In all cases a 15 mm free length of fabric was used between the matrix and the grips (Fig. 2b). This length was necessary for handling purposes. Load–slip curves were recorded and used to develop average pullout bond strength data. The bond was calculated by dividing the maximum pullout forces with the bundle perimeter and its embedded length, assuming circle bundle diameter. This implies an assumption that there is no penetration of the cement matrix in between the filaments of the bundle. The energy was calculated as the area under load-slip curves. Representative samples (with mechanical response close to the average as explained above for the tensile tests) were graphically compared. More details on pullout tests can be found in Ref. [4].

2.2.3. Restrained shrinkage samples

The restrained shrinkage samples were prepared by casting a cement paste directly on a corrugated steel section. The corrugated section of the steel served as restraint, so that the 'teeth' on the corrugated steel prevent shrinkage thereby restraining volume changes resulting in distributed multiple cracking (Fig. 3a). The steel restraining rack was 5 mm thick and 200 mm long to provide a high degree of restraint, which will also minimize bending due to the shrinkage of the cement paste. During casting a single layer of fabric was located in between two layers of the cement paste with a w/c of 0.42. The total height of the specimen was 20 mm. For comparison, plain paste samples were also prepared. The samples were demolded 24 h after casting and then dried at 50 °C for 24 h. During drying, cracks were developed across the surface in distributed manner as observed in Fig. 3b. Five samples were prepared for each tested system, of carbon fabrics and plain paste.

These specimens were used to generate multiple cracks in the specimen to study the influence of the carbon fabrics on crack pattern. The cracks here developed under restrain conditions during the first day from casting, providing relatively visible cracks, which could more easily used to measure crack width. These cracked specimens were used to study the fluid ingress of the carbon TRC elements with X-ray radiography using a contracting solution of 0.5 M lead nitrate.

2.2.4. Samples for controlled crack opening – wedge splitting test

A special mold was designed and built to produce samples with dimensions of 100× 100 mm and thickness of 10 mm (Fig. 4). The samples were prepared with a w/c of 0.42 and one layer of fabric located in the center of the sample. In each sample, two steel rods with diameter of 10 mm were used to hold the ball bearings during the wedge splitting test). The samples were demolded 24 h after casting. After demolding, a 3 × 30 mm notch was cut at the top of each sample (Fig. 5). Samples were then sealed in plastic sheet for 24 h and then used for experiment. Three samples were prepared for each carbon fabric type. For comparison another three samples with plain paste (no fabrics) were also prepared.

The wedge splitting specimens were used to generate cracks in the specimen so that the cracks could be imaged with X-ray radiography, to study the relationship between cracking and fluid ingress (of contrasting agent with 0.5 M lead nitrate). In this study the load was applied with the rate of 0.2 mm/min. An LVDT was glued to the surface of the sample as a way to measure crack opening displacement (COD). This provided slow crack growth that observed by X-ray imaging. Using this device, loading was stopped at two desired crack openings (0.03 mm and 0.3 mm). Once the load was stopped solution was added to the sample and the fluid ingress into the cracked sample was studied.

2.2.5. Fluid transport tests – X-ray radiography

X-ray radiography was used to study the fluid ingress of the carbon TFRC elements. The restrained shrinkage samples and the splitting wedge samples were tested for plain sample and the samples with the coated and non-coated fabric samples.

A GNI X-ray absorption system was used [10,11]. The distance between the source and the specimen was 200 mm resulting in each image capturing a 20 mm view with a pixel pitch of 12 pixel/mm. The X-ray was operated with a voltage of 40 keV, a current of 100 μA, and an integration time of 5 s. To image the entire restrained shrinkage sample the camera and source were moved in 18 mm increments, and the images were reassembled. For the wedge samples the sides of each sample were sealed with aluminum tape before ponding with the contrasting solution. For testing the restrained shrinkage samples, the sides of each sample were sealed with aluminum tape after oven drying and before ponding with contrasting solution. A contrasting agent was used (0.5 M lead

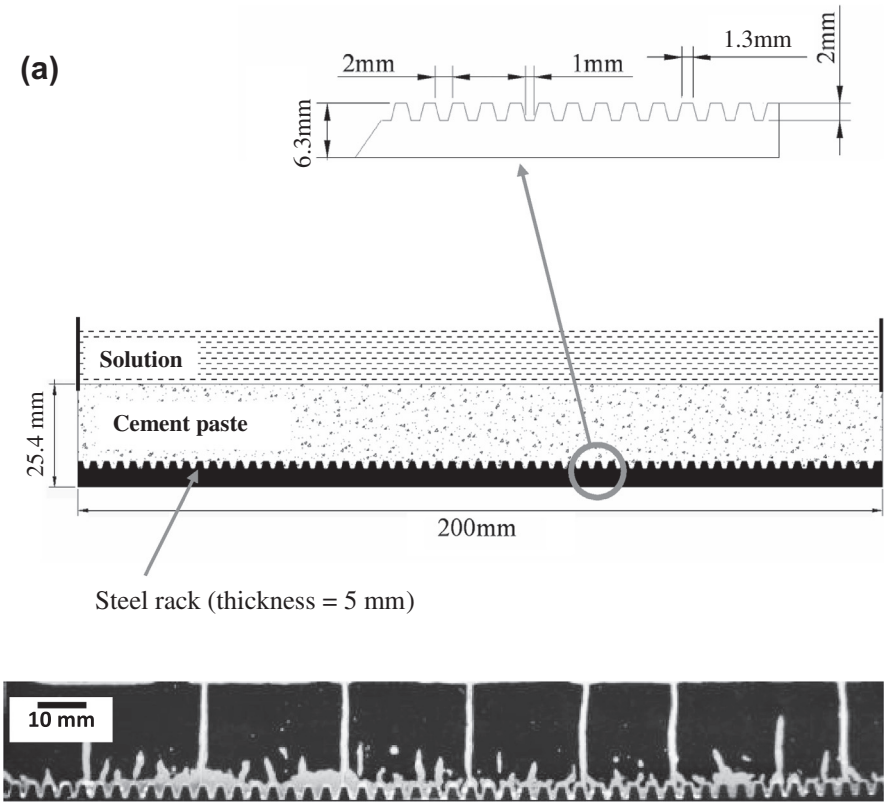

Fig. 3. (a) Schematic view of the steel rack used to induce multiple shrinkage cracks, as the solution was added after drying and cracking, and (b) typical image taken under UV light where fluorescent epoxy has penetrated the cracks (the fluorescent epoxy is shown as nearly white).

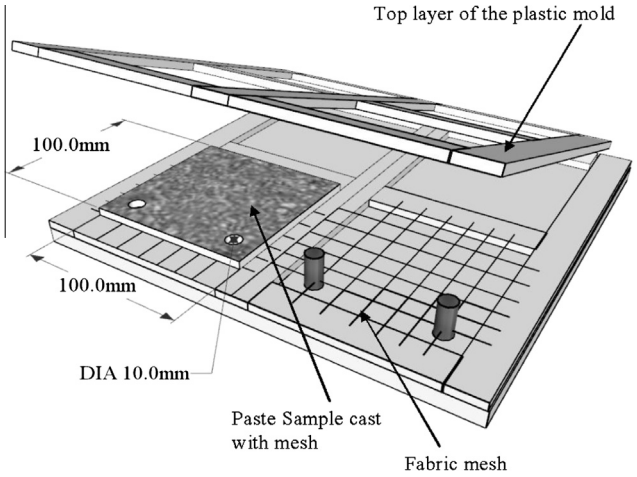

Fig. 4. Schematic view of the mold used to cast fabric reinforced samples for wedge test. The right hand side of the mold shows the mesh in the mold before the paste is placed while left hand side of the mold shows a completed specimen.

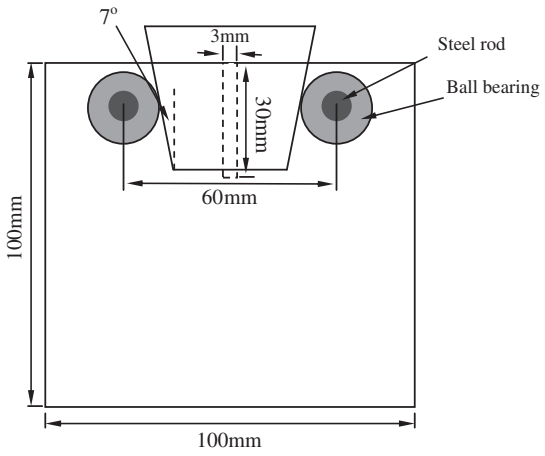

Fig. 5. A schematic view of the wedge test sample with a 3 × 30 mm notch.

nitrate) for both cases. The ponding time was ~15 min. More details can be found in Refs [12,13].

2.2.6. Microstructure characteristics

A Scanning Electron Microscope (SEM) was used to observe each system. The observations were focused on evaluating the composite cross section as well as the structure of the matrix along the yarn length in order to study the bond between the fabric and the cement matrix as well as the open spaces between the filaments of the bundle composed the fabric. It should be noted that a precision diamond tipped water cooled saw was used and the samples were not polished, to minimize damage of yarns, fabrics and interface.

3. Results and discussion

3.1. Mechanical properties

Fig. 6 presents the typical tensile response of the composites with the coated and non-coated carbon fabrics. The figure shows that the coated fabric composite performed much better than that of the non-coated fabric composite. Significant improvement is observed for all mechanical properties of the composite reinforced

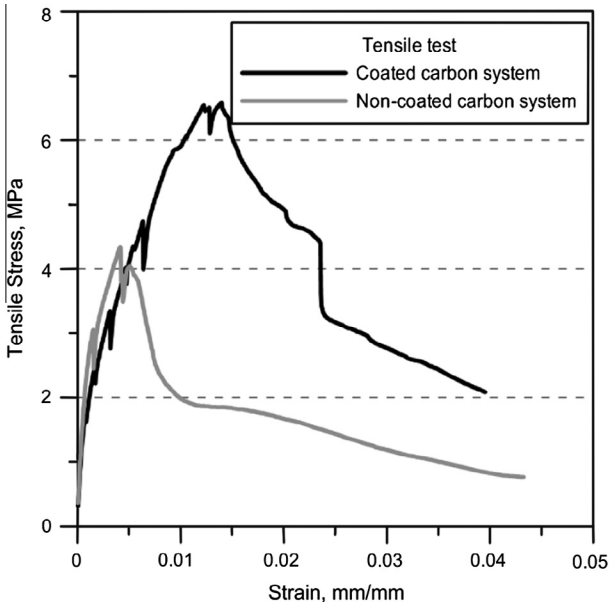

Fig. 6. Stress–strain curve of coated and non-coated carbon fabric reinforced composites.

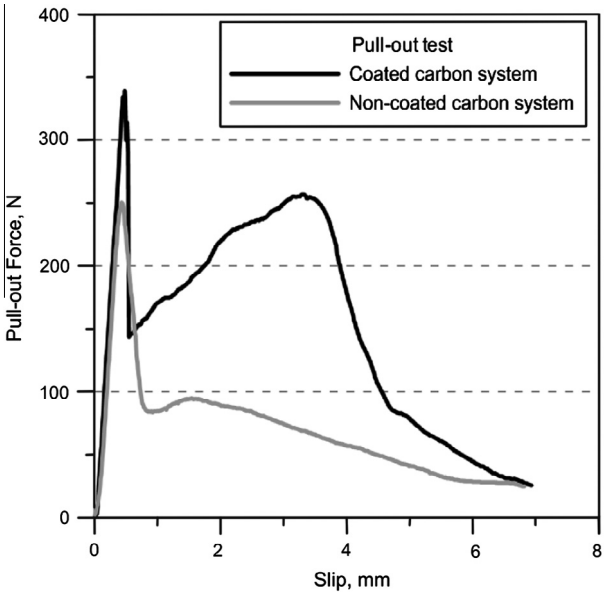

Fig. 7. Pull out force–slip curve of coated and non-coated carbon fabric systems.

with the coated carbon fabric, with 43% increase in ultimate tensile strength (UTS), 220% increase in elongation at UTS and 140% increase in energy absorption. The average tensile strengths of 5.9 MPa and 4.1 MPa and toughness values of 5.75 J and 2.38 J were calculated for the coated and non-coated composite systems, respectively. The coefficients of variance were approximately 15% for all systems. When comparing the shape of the tensile stress–strain curves of coated and non-coated carbon systems, a significant drop in tensile stress after reaching the peak is observed for the non-coated system, from above 4 MPa to about 2 MPa. For the coated system the reduction in stress after reaching the peak is more moderate. Such behavior of the coated system may suggest better reinforcing efficiency and bonding with the cement matrix. The coating improves the stress transfer between filaments within the bundle and their reinforcing ability when part of the cement composite as discussed above (Section 2.1). The bond between cement matrix and fabrics was studied by pullout tests as discussed in the following section.

Pullout tests were conducted for both tested fabric systems. In this test the whole fabric was pulled out from the cement matrix, containing 2 yarns along the pullout direction. Fig. 7 presents the pullout responses of the two fabric systems. The improved pullout behavior of the coated fabric system is clearly observed as compared with much lower pullout behavior of the non-coated fabric system. These results indicate improved bond strength when the bundles are coated, which suggests improved stress transfer between fabric and matrix. Bond strengths of 1.8 MPa and 1.4 MPa were calculated for the coated and non-coated fabric systems, respectively. The bond strength was calculated using the maximum peak (i.e., the first peak for the coated system in Fig. 7). Energy absorption values of 0.88 J and 0.37 J were calculated for the coated and non-coated fabric systems, respectively. This is consistent with an improvement in energy absorption for the coated fabric system as compared with the non-coated fabric system. These values highly emphasized the improved bonding between fabric and matrix when the bundles within the fabric were coated. Note that due to the coating, the filaments within the bundle are glued together; when loaded during pullout test the stresses are efficiently transferred to all reinforcing filaments within the fabric, exhibiting high pullout resistance and good bonding. However for the non-coated fabric the filaments are separated, when loaded the stresses do not transfer as efficient to the inner filaments of the bundle, as they transfer by friction only due to sliding of filaments against each other, exhibiting low pullout resistance and reduced bonding. Detailed discussion with observations on the microstructure of these systems is provided in Section 3.2.

Furthermore, the pullout responses behave differently when comparing the load-slip curves of the two tested fabric systems. For the non-coated system, the loads increase up to the peak with a significant sharp drop after reaching the peak load. Following this drop the load values are preserved which may suggest sliding of the inner filaments with hardly any change in the embedded length of the outer filaments, having direct contact with the matrix. Then, a continuous linear reduction in loads is observed, suggesting pullout of most filaments from the cement matrix, as the embedded length reduced. For the coated fabric system the pullout behavior is somewhat different. The loads increase up to the peak following with a sharp drop but to much less extent as for the non-coated system, i.e., with the coated system the drop in loads after reaching the peak is less significant. This suggests that the reinforcing coated bundle at this stage still carries significant amount of loads, as it behaves as a single reinforcing unit. After this drop, the load values are increasing reaching a second peak at much larger slip, i.e., the fabric keeps carrying the load, suggesting better stress transfer between bundles and matrix with improved reinforcing efficiency. Only after reaching the second peak, continuous linear reduction in loads is observed for the coated system, i.e., pullout of the bundles from the cement matrix. Such differences in pullout behavior indicate differences in bond mechanisms between the two fabric systems. The coated bundle behaves as a single reinforcing unit where all filaments are carried the loads [6], while for the non-coated bundle the filaments of the bundle act separately. The filaments that are in direct contact with the matrix carry most of the loads, while the inner filaments mainly slide against each other and therefore are less effective for reinforcement.

The improved bond strength and behavior of the coated fabric system correlates well with the tensile behavior, greater bond and reinforcing efficiency results in improved tensile behavior.

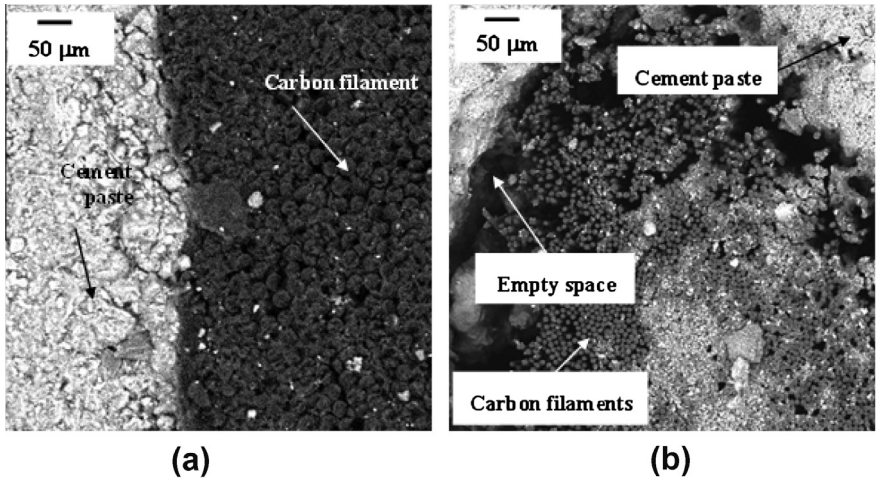

Fig. 8. Cross sectional image of carbon bundles with a Scanning Electron Microscope (SEM): (a) coated and (b) non-coated bundles.

3.2. Microstructure characteristics

The differences in bond strength and the related differences in tensile behavior of the two carbon fabric systems discussed above can be explained based on SEM observations. Scanning electron micrographs of the composites with the two different carbon fabrics are shown in Fig. 8. A compact and intimate interface is observed between the multifilament coated carbon fabric systems and the cement matrix, without visible voids and gaps at the interface bundle–matrix (Fig. 8a). In addition, a high degree of penetrability of the epoxy coating can be observed and no large empty spaces found between the filaments in the entire bundle (at the core of the bundle). Such compact and intimate interface with no gaps between bundle and matrix and within the filaments of the bundle is a clear evident for the good bond developed within this system, leading to the improved mechanical performance.

Conversely, for non-coated multifilament carbon fabric systems only partial penetrability of the cement matrix into multifilament bundle occurs and high empty space percentage can be observed as clearly shown in Fig. 8b. Also, large percentage of empty spaces can be seen in the interface area between the cement matrix and the multifilament bundle. Empty spaces between filaments of approximately 37% of the cross section area were calculated for each bundle embedded in the cement paste. This low cement penetrability and porous interface indicates poor bonding, leading to the low tensile and bond strength of the non-coated fabric system. These differences in microstructure between the two fabric carbon systems can also influence fluid ingress as will discuss later.

3.3. Cracking

The crack pattern and crack width that develop are highly dependent on the bond strength and bonding mechanisms and can provide more information of fabric and bundle treatment (coated or non-coated) influences on the overall mechanical behavior of the composite. The cracks can also influence the long term durability behavior of the TRC components due to their influences on fluid transport ability. In this study several methods were used to record and study crack pattern and cracking behavior: (i) cracks in the tensile specimens, (ii) cracks in the restrained shrinkage specimens, and (iii) single cracks opening carefully controlled by wedge splitting test.

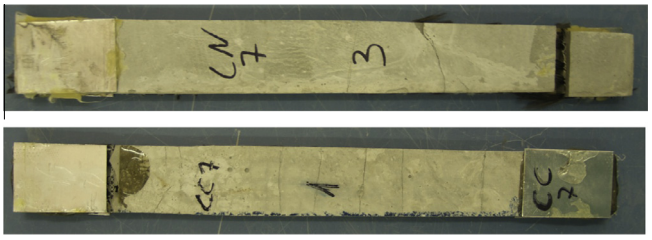

Fig. 9. Cracked samples after tensile tests: (a) non-coated and (b) coated of the carbon fabric composites.

3.3.1. Multiple cracking and crack width

During the tensile test multiple cracking was observed and recorded by a camera for both tested fabric systems (Fig. 9). It can be clearly seen that more cracks developed in the coated fabric composite during the tensile tests, observing seven average cracks for coated carbon samples while only two cracks for the non-coated fabric composite. The crack pattern is controlled by the bond that developed between fabric and matrix. A more dense crack pattern corresponds with better bonding due to improved stress transfer between matrix and reinforcement. In this work the coated fabric system exhibits a more dense crack pattern which is consisted with improved bond strength. This correlates with the pullout test results (Fig. 7), indicating stronger bond for the coated fabric system.

Multiple cracking was also observed for the restrained shrinkage samples. After cracking the restrained shrinkage samples were impregnated with fluorescent epoxy and imaged using optical fluorescent microscopy (i.e., UV light). The crack pattern was recorded for the different systems presented in Fig. 10. From each sample five cracks were selected and the width of each crack was measured at ten different locations along the crack. The selected five cracks were taken from the cracks that developed through the entire thickness of the specimen. Fig. 11 shows one of the five cracks used to measure crack width along with the average measured crack width for the three examined systems. Fig. 10 indicates more dense crack patterns for both fabric systems as compared with the plain matrix. No significant difference is observed when comparing the coated and non-coated fabric systems. This may be due to the fact that the crack pattern is relatively dense and the restraint provided by the bar along the base of the sample limits the width of the crack that forms. When observing the coated fabric system in more details,

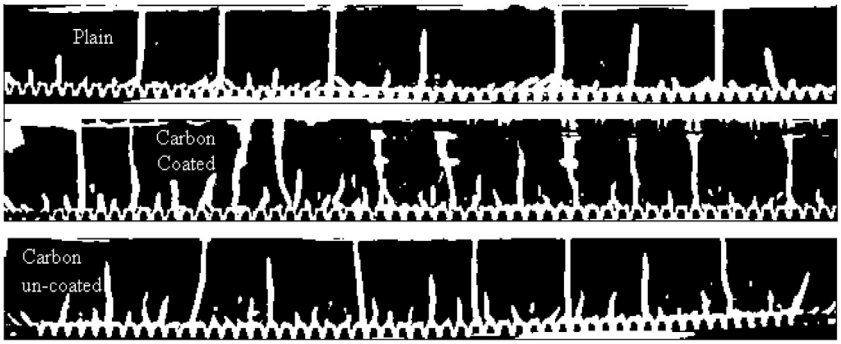

Fig. 10. Crack pattern in the restrained shrinkage specimens, plain specimen and the specimens with coated and non-coated carbon fabrics. The images are taken under UV light where fluorescent epoxy has penetrated the cracks (the fluorescent epoxy is shown as nearly white).

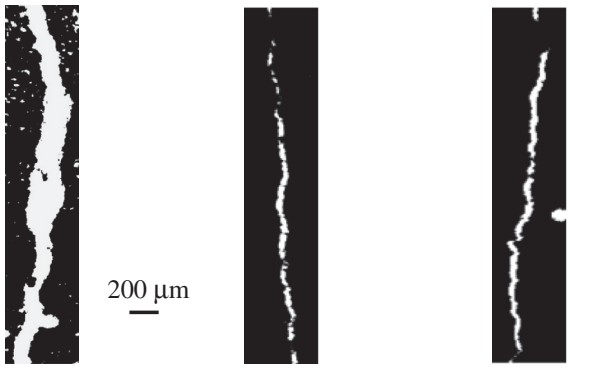

Fig. 11. Typical crack in the restrained shrinkage specimen, plain specimen, and the specimens with coated and non-coated carbon fabrics. The images are taken under UV light where fluorescent epoxy has penetrated the cracks (the fluorescent epoxy is shown as nearly white).

some of yarn junctions within the fabric are well recognized, as penetrability of epoxy is observed also along the bundle and not only through the cracks. This may suggest debonding between the coated bundle and matrix during shrinkage. Such debonding mechanism may also develop during pullout tests which may lead to the second peak observed for the coated carbon system presented in Fig. 7. This behavior is not observed for the non-coated fabric system.

The plain matrix (without fabric) exhibits a larger crack width (175.5 μm) as expected, as in this case there is no bridging of the crack and the width is limited by the restraining fabrics. No significant difference in crack width was measured between the two fabric systems, similar values of 38.4 μm and 35.5 μm were measured, for coated and non-coated, respectively.

The crack pattern as well as the size and width of the crack expect to influence the transport properties of the system.

3.3.2. Controlled single cracking

A splitting wedge test was used to open a single crack. The crack was induced under carefully controlled conditions while using X-ray experiment, simultaneously. This allows observing the crack by X-ray imaging during loading. Samples of plain cement paste and the two fabric systems were tested. For each examined system two samples were imaged with two different crack openings of 0.03 mm and 0.30 mm. The single crack opened by the wedge test is presented by radiograph images in Fig. 12. The cracks become visible as darker sections of the image due to the presence of contrast solution that penetrated through the cracks.

The radiograph images of the cement paste samples are presented in Fig. 12a for both crack openings. The cracks can clearly be seen in both cases, which mean that the solution can easily penetrate into the entire length of the cracks. The differences in crack opening are obvious by naked eye, thinner for the 0.03 mm and wider for the 0.30 mm wide cracks. For the cement paste in both crack opening systems only one crack is develop and the crack is relatively straight with no branches, starts from the bottom of the saw cut and propagate to the bottom of the sample.

The radiograph images of the wedge splitting samples contained coated and non-coated carbon fabrics exposed to the contrasting agent are shown in Fig. 12b and c, respectively. Also here the cracks are clearly seen but here more than one crack is observed and the crack pattern is more complicated. The crack starts from the bottom of the cut saw but the propagation of the crack is not in a straight path from top to bottom as for the plain paste. Here the crack propagates in a more complex path, growing also along the width and not only along the length of the specimen. Such crack behavior can be observed for both crack openings and fabric systems, coated and non-coated (Fig. 12b and c). When comparing the images of the two crack openings, 0.03 and 0.30 mm of the two fabric systems, the difference in the opening of the crack is mainly due to development of several close parallel cracks, with more cracks for the wider crack opening system and less for the thinner crack opening, especially when comparing the coated fabric system (Fig. 12b). This means that during loading and crack growth the measured crack opening is mainly by development of new cracks, which may suggest fabric bridging mechanism. Moreover, when comparing the crack pattern of the two fabric systems (coated and non-coated, Fig. 12b and c, respectively) clear branching of cracks is observed for the coated fabric, especially for the large crack opening sample of 0.30 mm. For the non-coated fabric system fewer crack branches are visible. The branching pattern suggests that the coated fabric bridging and restraining the cracks in a better manner than the non-coated one, due to stronger bonding between fabric and matrix as also obtained by the pullout test (Fig. 7).

It can be concluded based on the above discussion that the carbon fabrics allow better restraint of the developed cracks leading to more but finer cracks as compared with the plain cement paste. The coated carbon system provides finer but more cracks compared with the non-coated carbon system due to improved bonding, as the cracks are split and branched during loading. The fine but increased number of cracks should be considered when dealing with fluid transport as discussed in the following section.

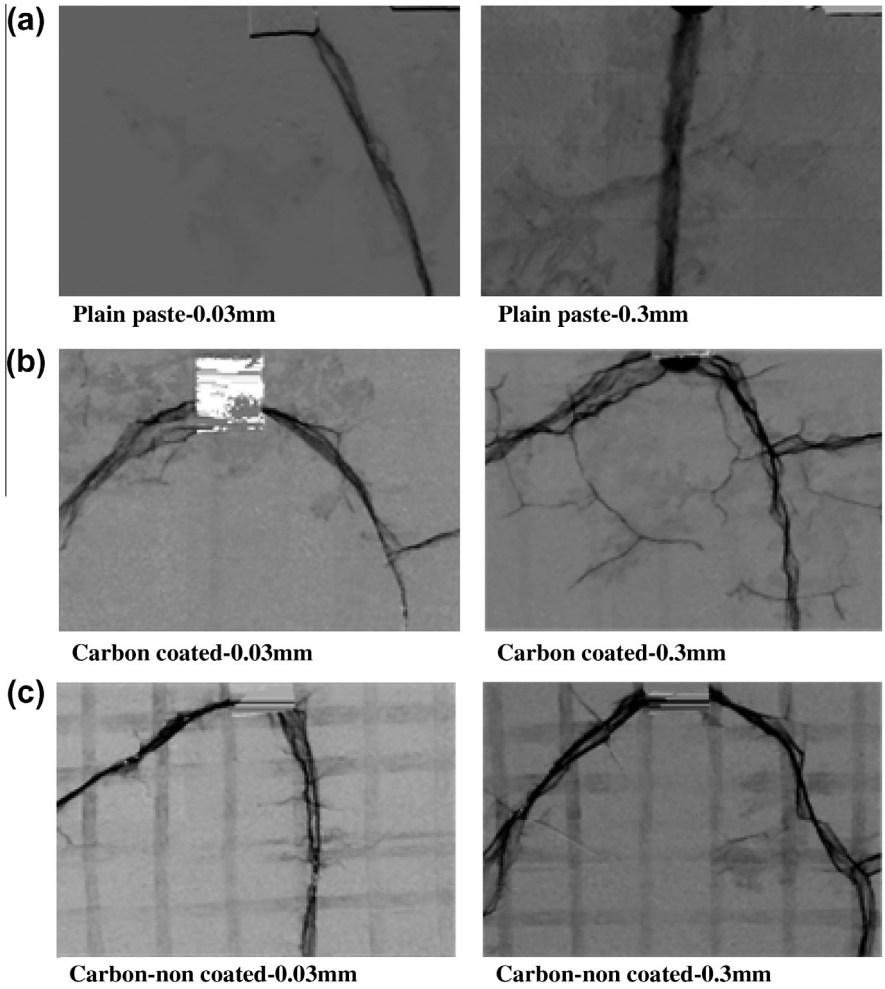

Fig. 12. X-ray radiography images of wedge test samples (a) plain paste, (b) coated carbon composite and (c) non-coated carbon fabric composite after ponding with contrasting agent at different crack openings. The dark portions of the image show less X-ray transmission and denote where the crack has been filled with the contrasting agent.

3.4. Fluid transport

When dealing with TFRC, not only should the mechanical performance of the composite be considered but the transport characteristics as their influence on durability of the final product should be considered. It is well known that fluid transport is significantly dependent on crack pattern and crack width. When textile fabrics are used as reinforcement for cement matrices usually the crack width is relatively small with dense crack network as discussed above (Figs. 10 and 11), and therefore expected to improve the durability of the TFRC product. However when dealing with TFRC, besides crack width and crack pattern also the gaps and empty spaces between filaments due to the unique multifilament nature of the textile reinforcement should be taken into consideration. In this work the fluid transport was studied for the coated and non-coated fabric composites and compared with plain cement matrix. The fluid transport was measured by X-ray radiography, for the samples cracked by the splitting wedge test and in the shrinkage test. The portion of the specimen that has been penetrated with the contrasting agent appears darker or nearly black when observing the radiograph images.

For the wedge test specimens after loading was performed, the load was held constant and a contrasting agent was pond on top of the sample. The load was stopped at two specific crack openings (0.03 and 0.30 mm). At these specific points the fluid transport was imaged using the X-ray radiography, for the carbon fabric systems and plain paste (Fig. 12). For the plain paste system, with crack opening of 0.03 mm, the contrasting agent fluid observed only inside the cracks but not in the bulk paste matrix. However some changes in color, i.e., darker color, are seen at the paste bulk for the large opening crack system of 0.30 mm, suggesting slight penetrability of solution into the paste (Fig. 12a). Similar changes in color are observed within the paste for the coated fabric system in both systems (Fig. 12b), implying penetration of solution in both cases into the bulk paste.

For the non-coated fabric composite the situation is quite different. When observing the bulk paste region (i.e., away from the cracks) the yarns of the fabric are clearly visible at both crack openings, of 0.03 mm and 0.30 mm (Fig. 12c). This means that for the non-coated fabric system the solution penetrates along the yarns for both crack opening systems. The contrasting agent penetrates from the ponding region through the perpendicular multifilament yarns into the specimen. In this case the filament bundles contain a large volume of empty spaces (Fig. 8b). Note that for the coated carbon fabric (Fig. 12b) the yarns are hardly visible (only very light yarns are seen within the bulk paste region) even for the wide crack system of 0.3 mm. Based on these results it can be concluded that the multifilament yarns transport the fluid into the composite due to the empty spaces between the filaments, this pronounced when the bundle is not coated. Such fluid transport does not

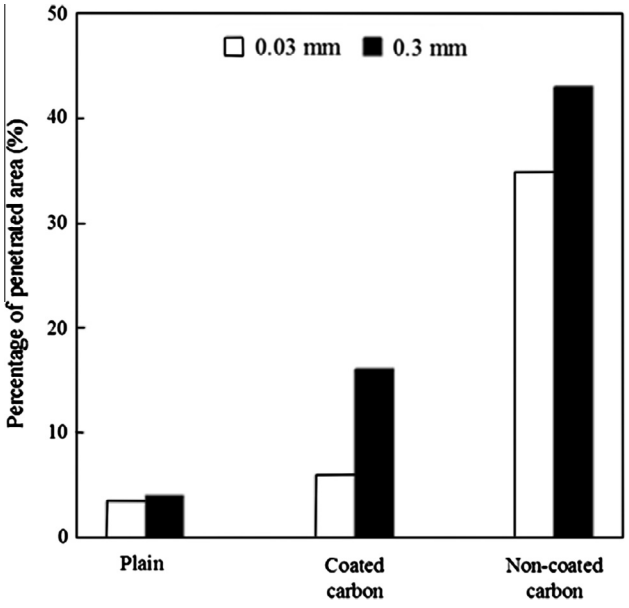

Fig. 13. Percentage of the sample that has been penetrated by water for wedge test samples with different crack openings.

necessarily depend on crack width but more on yarn treatment. Therefore, fabric made using fully coating yarns exhibits very low fluid transport along the bundle while for the non-coated fabric the fluid transport is much higher along the filament of the bundle.

To better understand the influences of the fabrics on fluid transport behavior, the fluid penetrated area of all systems were calculated and the results are presented in Fig. 13. To determine the percentage of each image that was infiltrated by the solution, an algorithm was applied using ImageJ. A threshold was applied to the image to separate the dark (wet) and light (dry) portions (i.e., the portions of the specimen) and then the percentage of dark region was determined as shown in Fig. 13. The wet area of the sample is relatively large for the non-coated carbon system for both crack openings. Again, this can be attributed to the fluid transport through the empty spaces between bundle filaments of non-coated carbon fabric. For the coated carbon system a much lower are that has wetted is observed when compared with the non-coated system, as expected due to coating. However, a significant increase in wetted area was calculated when the crack was opened from 0.03 mm to 0.30 mm. It may suggested that this increased in wet area while opening the crack of the coated system is due to development of more cracks including branches as shown in Fig. 12b. This crack branching may allow ingress of fluid into the bulk paste as observed for both crack openings of the coated system (Fig. 12b). When the crack is highly opened more and wider cracks and crack branches are developed leading to more massive fluid ingress through the cracks and into the bulk cement paste as reported in Fig. 13.

In the case of the plain cement matrix, the area penetrated by the solution is significantly smaller than both carbon systems (Fig. 13). This is due to fluid penetration that occurs through the cracks in the sample, while in both carbon systems fluid is transport through the yarns and through the cracks compared with that of plain paste. When the two carbon systems are compared, the non-coated carbon shows higher wetting due to presence of empty spaces within the bundles, and debonding. However some tiny empty spaces are remained also within the coated bundle as the coating is not completely perfect, allowing same transport of fluid also for the coated system.

A similar trend is also observed when examining the restrained shrinkage specimens ponded with the contrasting agent (Fig. 14). This figure shows radiography images of the multiply cracked samples of plain paste and the two carbon systems after 1 min and 45 min from ponding. Fig. 14a shows radiography image of

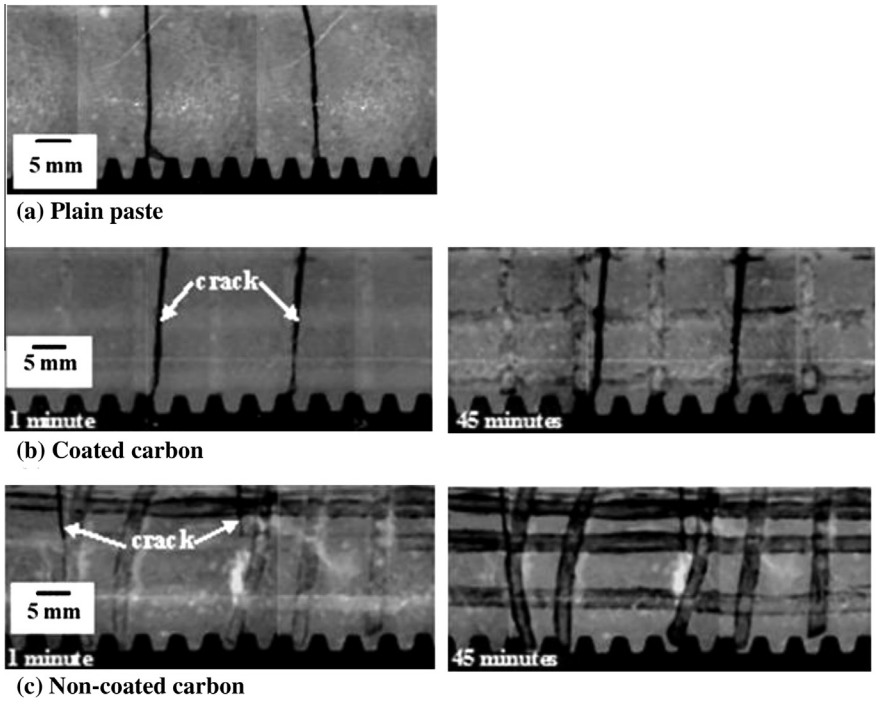

Fig. 14. X-ray radiographic images of restrained shrinkage samples ponded with the contrasting agent: (a) plain paste after 45 min ponding, (b) coated carbon after 1 min and 45 min ponding, and (c) non-coated fabric 1 min and 45 min ponding. The dark portions of the image show less X-ray transmission and denote where the crack has been filled with the contrasting agent.

multiple cracked plain paste specimen after 45 min of ponding with the contrasting solution. The cracks are clearly observed due to penetration of the solution through their entire length. However penetrability is not observed at the paste bulk. Similar observation of clear full length cracks without penetrability into paste is seen for the coated carbon system after 1 min from ponding (Fig. 14b). However 45 min after ponding, besides cracks it is also possible to see slight penetrability of the contrasting agent along the yarns of the fabric (Fig. 14b) which are not visible after 1 min from ponding.

For the restrained shrinkage samples with the non-coated fabric (Fig. 14 c), the filaments of the bundle yarn are visible even at short duration from ponding (1 min), i.e., the contrasting agent penetrates along the yarns almost immediately after ponding. The penetration of the solution along the filaments of the bundle is even more pronounced 45 min after exposure. The presence of the contrasting solution within the bundles can be easily seen as the contrasting agent possibly penetrates from the ponding region through the perpendicular multifilament bundles into the entire specimen.

In addition, for the non-coated system, at short durations after ponding hardly any cracks are observed, only very small at top zone of the specimen (Fig. 14c). This is contrary to the plain paste and the coated carbon specimens (Fig. 14a and b respectively), where full length cracks are clearly observed along the entire thickness of the specimens. This may indicate that the cracks for the non-coated carbon are too thin, with average of 35.5 μm, for the solution to easily penetrate into the entire crack length. This means that the solution can easily penetrate into the entire length of the cracks for the coated carbon system but not for the non-coated carbon system. However, the fabric made of fully coating bundles exhibits very low rate of fluid transport as the non-coated fabric wet almost immediately after exposure. This may indicate that the rate of fluid ingress is depended mainly on surface treatment, coated vs. non-coated and much less on crack width when multifilament textiles are used as reinforcement.

This trend is clearly observed in Fig. 15, which shows the fluid penetrated area vs. the duration of time since the contrasting agent was added. The wet area of the sample influenced by the contrasting agent was relatively large for the non-coated carbon system. The large area that has been penetrated is seen for all exposure periods, however there is a steady increase over time likely due to absorption from the surfaces as well as from along the filaments. A noticeable increase in wetting area is also observed for the coated carbon fabric system but with much smaller penetrated area. This may suggest that although most of the gaps between filaments are filled with coating and therefore this system behaves similar to the cement paste, some tiny empty spaces are remained within the bundle, allowing slow transport of fluid during time. The X-ray radiography images were acquired with a 15 min time interval for approximately 45 min after ponding. To determine the percentage of wet area of each image an algorithm was applied using ImageJ.

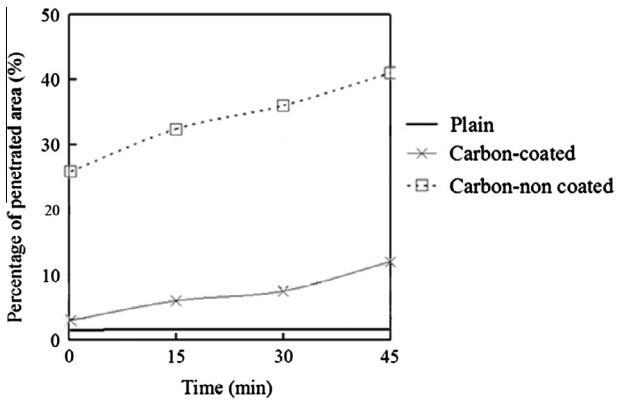

Fig. 15. Percentage of the area of the specimen that has been penetrated by (wetted area) the contrasting agent vs. time for the shrinkage samples.

It can be summarized that the transport behavior of the multiple cracked samples (restrained shrinkage) is similar to that of the single opened crack (by splitting wedge test); transport of fluid only through the cracks of the plain paste system while for the textile systems the fluid can transfer also along filaments of the bundle with more significant fluid ingress rate of the non-coated system. However the carefully controlled conditions for opening the single crack under the wedge test, leads to development of a large number of finer cracks including crack branching of the fabric systems which also contribute to fluid ingress.

4. Summary and conclusions

In general, carbon textile fabrics improve the mechanical performance of cement-based composites. The carbon fabrics have a strong bond with the cement matrix which leads to a finely distributed crack network. Fluid transport in the cracks and along the filaments is dependent on crack pattern, crack width, and filament bond. The goal of this work was to demonstrate the importance of bundle coating on composite mechanical behavior, bonding, and fluid transport.

It was shown that coated carbon bundles increase the tensile properties of the textile cement-based matrix with respect to UTS, elongation at UTS, and energy absorption. The coating on the fabric decreases the empty spaces between filaments and provides more intimate interface between matrix and bundle which improved stress transfer as confirmed by pullouttests and SEM observations.

TFRC specimens with coated carbon bundles exhibit a more dense crack pattern during tensile testing and a more branched crack pattern during splitting wedge test of a single crack as compared with the non-coated system. Such a fine crack pattern can be due to more efficient bridging and restraining of the developed cracks by the stronger bonding, leading to improved mechanical performance. However, these additional fine cracks were found to influence and increase fluid ingress into the composite as compared with plain cement paste. This increase in fluid ingress due to crack branching can decrease durability properties of TRC elements. However, the size and width of the cracks also influence durability, as these are smaller for TRC systems.

The samples with relatively large crack width, greater than ~40 μm, permitted fluid to penetrate the sample through the crack and crack face. This was the case for the samples of plain cement matrix. Conversely, in case of both carbon systems the cracks were much finer and less than ~40 μm. Some fluid penetrability was observed into the bulk specimen in both carbon systems, coated and non-coated, even in cases where the fluid was not fully permitted to enter along the entire crack length. This was due to the ingress of fluid along the bundles of the fabrics through the open space in between the filaments. Whereas the non-coated carbon permit a rapid fluid ingress through the open space in between the filaments of the bundle, the fully coated carbon bundles showed much lower fluid ingress along the bundles. This can be attributed to less empty space between filaments.

Therefore when durability is considered for textile–cement composites it is necessary to take into account the coating of the yarns composed the fabric and crack pattern as they influence the fluid transport properties.

It can be concluded that the coating of carbon fabric has a beneficial influence on both mechanical performance and resistance to

fluid ingress. The coating increases the mechanical properties and decreases the fluid transport properties. The decrease in fluid transport is due to the fact that the coated fiber has less empty space within the bundle and good bonding as compared with non-coated fabric, thus leading to improved mechanical behavior and durable TRC elements. It should be noted that such polymer coating is stable at regular service environment and temperatures but not necessarily at elevated temperatures such as caused by fire.

Acknowledgments

The authors would like to thank the Textile and Civil Engineering Departments at the Technical University of Dresden Germany (Technische Universität Dresden) for providing the carbon fabrics for this work including their performances.

References

[1] Brameshuber W, editor. Textile reinforced concrete – state of the art report, RILEM Technical Commitee 201-TCR; 2006.
[2] Bentur A, Mindess S. Fiber reinforced cementitious composites. 2nd ed. UK: Taylor and Francis Group; 2006.
[3] Mobasher B. Mechanics of fiber and textile reinforced cement composites. CRC Press; 2011.
[4] Peled A, Bentur A. Fabric structure and its reinforcing efficiency in textile reinforced cement composites. Composites Part A 2003;34:107–18.
[5] Peled A, Mobasher B. Tensile behavior of fabric cement-based composites: pultruded and cast. ASCE J Mater Civ Eng 2007;19:340–8.
[6] Krüger M, Xu S, Reinhardt, Ožbolt HW. Journal of experimental and numerical studies on bond properties between high performance fine grain concrete and carbon textile using pull out tests. In: Beiträge aus der Befestigungstechnik und dem Stahlbetonbau (Festschrift zum 60. Geburtstag von Prof. Dr.-Ing. R. Eligehausen), Stuttgart; 2002. p. 151–64.
[7] Zhu D, Peled A, Mobasher B. Dynamic tensile testing of fabric-cement composites. Constr Build Mater 2011;25(1):385–95.
[8] Mechtcherine V. Towards a durability framework for structural elements and structures made of or strengthened with high-performance fibre-reinforced composites. Constr Build Mater 2011:93–104.
[9] Mechtcherine V, Liebold M. Permeation of water and gases through cracked textile reinforced concrete. Cem Concr Compos 2011;33(7):725–34.
[10] Nielsen GG. X-ray CT system – users manual. GNI/XRAS/UM.003; 2007.
[11] Paradis F, Weiss WJ. Using X-ray tomography to image cracks in cement pastes. In: International conference on high-performance fiber-reinforced concrete composites (HPFRCC), Stuttgart, Germany; 2007.
[12] Poursaee A, Peled A, Weiss WJ. Cracking and fluid transport in coated and non-coated carbon fabrics in fabric reinforced cement-based composites. In: Brameshuber W, editor. Proceedings RILEM international conference on textile reinforced concrete, September, Aachen, Germany; 2010. p. 257–70.
[13] Pourasee A, Peled A, Weiss WJ. Fluid transport in cracked fabric reinforced cement-based composites. ASCE J Mater Civ Eng 2011;2:1238–77.